Chemical Physics Letters 720 (2019) 113–118

Contents lists available at ScienceDirect

Chemical Physics Letters

journal homepage: www.elsevier.com/locate/cplett

Research paper

Special aspects of the thermodynamics of formation and polarisation of Ag/Si nanoparticles

A.V. Nomoev[a,*], N.A. Torhov[b], E.Ch. Khartaeva[a], V.V. Syzrantsev[a], N.V. Yumozhapova[c], M.A. Tsyrenova[c], V.N. Mankhirov[a]

[a] Institute of Physical Materials Science, Siberian Branch of the Russian Academy of Sciences, Sakhyanovoy str., 6, Ulan-Ude 670047, Russia
[b] Tomsk State University, Lenina av., 30, Tomsk 634050, Russia
[c] Buryat State University, Smolina str., 24a, Ulan-Ude 670000, Russia

HIGHLIGHTS

- We found the diffraction fringes in the nano Ag-Si is caused by eutectic decomposition into their layers.
- We showed the cooling rate determines the formation of layered or globular eutectic compounds.
- We showed the cooling rate rules the size of eutectic plates and the size of Ag-Si nanoparticles.

ARTICLE INFO

Keywords:
Nanoparticle
Diffraction fringes
Eutectics
Structure
Dipole moment

ABSTRACT

An analysis of the mechanism of formation of composite nanoparticles of Ag/Si shows that it depends on their stoichiometric composition, conditions of condensation and crystallisation. During the crystallisation of the nanoparticle core, eutectics consisting of silver and silicon layers are formed. Diffraction fringes in the nanoparticle core are caused by the formation of eutectic platelets during crystallisation of phase components. Layers of the conductor Ag and semiconductor Si form, creating an electric charge at the boundaries. We demonstrate the dependence of the sizes of these Ag/Si nanoparticles on the rates of heating and cooling of the materials during synthesis.

1. Introduction

Two-component nanoscale systems with unique electromagnetic, optical, catalytic and other properties are of interest to research scientists around the world, as evidenced by the large number of publications in this area [1–3].

The formation of the structure of such nanoparticles is primarily determined by the methods and conditions of synthesis, which should allow us to combine the two materials even if they are immiscible in the bulk state. Physical methods such as the gas phase method [4–6], laser ablation [7–9], magnetron-sputter gas-phase condensation [10] and electric wire explosion [11] have been developed. When these methods are combined with the possibility of rapid heating and evaporation of both materials and the possibility of rapid controlled cooling of the resulting vapour mixture, the formation of nanoparticles with a complex structure occurs.

Of special interest are compositions of materials that are immiscible in the bulk state, such as Ag/Si [5], Ag/Cu [7], Mo/Cu [4], Au/Co [12] and others.

The high sensitivity of Ag/Si nanoparticles to microwave and THz electromagnetic fields determines their efficiency in technologies in which they are the main active elements of solid-state nanosystems controlled by radiophysical methods.

Their small size, high sensitivity and low power consumption also make them promising as active pixel elements of flexible radiation-resistant high-resolution displays, active vision radio systems and memory elements. The increase in spectral sensitivity and the efficiency of absorption of electromagnetic energy by Janus-like nanoparticles is ensured by the presence of two additional degrees of freedom, arising from a significant dipole electric moment, and an internal capacitance arising from the space charge region at the interface of the materials. This allows Janus-like nanoparticles of the same size and mass to absorb significantly more energy from electromagnetic waves than other types of nanoparticles.

* Corresponding author.
E-mail address: nomoevav@mail.ru (A.V. Nomoev).

https://doi.org/10.1016/j.cplett.2019.02.015
Received 9 January 2019; Received in revised form 6 February 2019; Accepted 6 February 2019
Available online 16 February 2019

Due to the fact that silicon and silver have different chemical natures, charge separation occurs in the core of an Ag/Si nanoparticle, which leads to the emergence of a large dipole moment.

This study aims to clarify the mechanism of formation of the core structure of Ag/Si nanoparticles, taking into account the crystallisation of the phase and structural components in the diagram of the Ag–Si phase rules [13]. A study was therefore conducted of the relationship between the size, structure, morphology, and phase composition of nanoparticles for laser ablation methods and the gas-phase method of electron beam evaporation.

2. Experimental

We describe the setup involving an electronic accelerator that was used for the evaporation of copper. Samples of Ag and Si were placed in a cylindrical graphite crucible. The crucible was then placed into a stainless steel chamber which was water-cooled. A 1.4 MeV electron beam with a current of between 3 and 15 mA and power of up to 1 MW/cm^2 was focused on the layers of Si and Ag. Less than 10 min after exposure, the components had completely homogeneously melted, and the mixture had vaporised. The vapors were then transported by argon gas from the evaporation chamber to a condensation chamber, where the they condensed into nanoparticles that were caught in a filter. The flow rate of the carrier gas was controlled by a fan built into the closed path of the gas. The details can be found in [5].

For the laser ablation method, we used a pulsed ytterbium infrared laser with power 20 W, wavelength 1064 nm and pulse repetition rate 60 kHz, which were regulated by a separate control unit. The laser radiation was focused on a target sample using a collecting lens, which was placed at the bottom of a cylindrical container with heptane.

Repeated scanning of a local surface area of the samples was carried out over 30 min. The use of this scanning system made it possible to evaporate the material evenly from the target surfaces, thereby reducing the formation of craters, increasing the ablation efficiency during prolonged irradiation and narrowing the size variation of the resulting nanoparticles.

3. Results and discussion

The characteristics of the obtained nanoparticles were determined using the methods of transmission electron microscopy (TEM) and electron diffraction of certain areas (HRTEM, SAED).

The components of the Ag-Si system do not interact with each other at a temperature below the liquid line (835 °C), according to the phase rule diagram (Fig. 1). In the particles obtained by electron-beam evaporation, the total immiscibility of the components in the solid state during the process of the crystallisation leads to their separation into the phase components Ag and Si and formation of a layered structure of the conductor and semiconductor (Fig. 2).

Let us now consider the process of crystallisation of the nanoparticle core, which contains Ag and Si, following the Ag-Si phase diagram. During the cooling and formation of the composite nanoparticles consisting of Si and Ag, the primary crystallisation of either silicon or silver takes place, depending on the stoichiometric composition of the nanodroplet formed. When the silicon content in the nanodroplet is higher than 11 at.%, nanoparticles with separate primary crystals of Si can be observed. In the case where the Ag content is higher than 89 at.%, the nanodroplet contains silver as the primary phase component. At a temperature of 835 °C, the residual of the liquid phase of the eutectic composition undergoes decomposition into a mechanical mixture of components: 89 at.% of Ag and 11 at.% of Si. The structure of this mixture with hypoeutectic composition contains primary crystals of silicon, a crystallising liquid melt and a eutectic system E(Si + Ag). The eutectic composition contains only E(Si + Ag). The proeutectic composition contains primary crystals of Ag and E(Si + Ag).

In our opinion, the formation of diffraction fringes in the nanoparticle core is the result of eutectic decomposition $L \xrightarrow{835^{\circ}C} E(Si + Ag)$ into platelet phase compounds of silver and silicon. Fig. 3 is a schematic view of the layers of the phase structural components, i.e. the silver and silicon platelets at the core of the Ag/Si nanoparticles.

In our experiment, wide and narrow diffraction fringes are observed in the TEM image of nanoparticles Ag/Si (Fig. 2b), the sizes of which depend on the cooling rate. The components of the eutectic may be formed as individual alternating phase layers, via a type of pearlite-troostite decay, or as coagulated phase precipitates, via a type of bainitic transformation in steels (granular pearlite) [14].

Nanoparticles of Ag/Si obtained using laser ablation are condensed and solidified directly in the liquid, which has high rates of heat removal and cooling compared to the inert gas used as a transport gas in the formation of the nanoparticles under the electron beam [5].

The main difference between pulsed laser irradiation and other synthetic methods is that in the former, the materials can be heated to a temperature that is higher than the melting point, whereas under normal experimental conditions the temperature is much lower and particles can be heated only to the melting point. Pulsed heating (on the ns scale) leads to very fast heating and to a high kinetic energy of the atoms. As a result, mutual diffusion takes place, giving rise to the formation of a metastable phase [8].

Fig. 4 shows the data for the laser ablation experiments. EDS X-ray microanalysis showed an Ag/Si ratio that is far of balance value. As mentioned earlier, nanoparticles with separate primary crystals of Si can be observed. Fig. 4b shows that the particles have a log-normal distribution and an average size of about 25 nm.

It is known that the time required for phase separation does not exceed 1 μs, as the diffusion rate increases significantly with increasing temperature. Due to this rapid quenching, atoms cannot be ejected from the crystal lattice during the crystallisation process. This situation can be compared to a quenching process, in the sense that atoms are “frozen” rapidly into a metastable state before an equilibrium condition (such as a phase separation) is reached [8].

In electron beam evaporation experiments, the cooling/solidification process takes about 0.1–1 s, and exceeds the phase separation time. In laser ablation experiments, the very fast cooling/solidification process takes about 10^{-5}–10^{-6} s [9].

An important aspect of the formation of nanoparticles obtained by gas-phase synthesis lies in the fact that in the process of their transition into the solid state, the cooling rate is not equal for every particle in the nanopowder, due to the differences in their size range, which can reach 10 nm or more. This is why the structure (the size of the platelets forming the eutectic) of the nanoparticles’ core and their morphology in the same nanopowder will differ greatly. Since the cooling inside the nanoparticle is irregular, the sizes of the diffraction fringes also vary.

The regularity and alternation of the diffraction fringes at the core of the nanoparticles is due to the formation in the system of the equilibrium phase components, which occurs in the process of interdiffusion of atoms and the formation of individual platelets of Ag and Si with minimum free energy.

The gas-phase method gives a similar TEM image of the Ag/Si nanoparticles, with the same diffraction fringes and composition of elements (Fig. 5a). However, in this case, the particles are larger and show a wider size distribution than for laser ablation (Figs. 4b and 5b). This can be explained by the low cooling rate.

By varying the electron beam current and the cooling flow rate, we obtain the dependencies of the average particle diameter. Since the electron energy is constant, an adjustment to the current of the electron beam gives a directly proportional adjustment in the power. It has been established that with an increase in the current of the electron beam, the average particle size increases (Fig. 6a). This is due to the increase in the concentration of evaporated substances, which affects the growth of the particles, as well as the enhancement of the liquid-drop

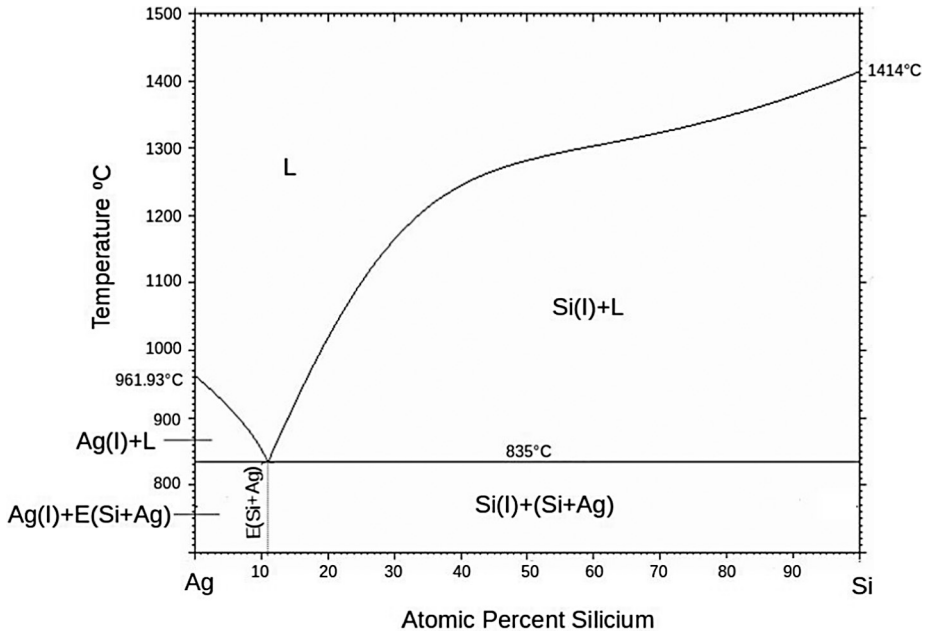

Fig. 1. Si-Ag phase diagram [13].

evaporation mechanism.

Fig. 6b shows the effect of the cooling flow rate on the particle size. With an increase in consumption, the average particle size decreases, due to the intensity of cooling and a reduction in the residence time of particles in the high-temperature zone where particles form [15].

Since the Ag-Si system has no conditions for the formation of solid solutions, Guinier-Preston zones or other non-equilibrium structures [16], it seems possible that the diffraction fringes are conditioned only by eutectic decomposition into two compounds of silver and silicon. A high resolution TEM analysis (HRTEM) of the Ag/Si nanoparticle core shows that it contains some silver with defective structures [9]. This is connected with the non-equilibrium residue of silicon in the crystal structure of Ag at the phase boundary, which can be seen in the diffused interface of the diffraction fringes in their TEM images [16].

In the process of formation of eutectic platelets of metal with semiconductor in the Ag/Si core, charge separation may occur at the boundary between these and the Schottky barrier. It is reasonable to assume that a large number of contacts between the conductor and the semiconductor at the Ag/Si boundary leads to a high total potential (Fig. 7) and the formation of the resulting vector (sum vector) of the electric field intensity, $\Delta\bar{E}$.

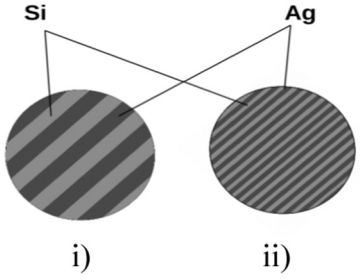

Fig. 3. Schematic view of the size of the diffraction fringes of Si and Ag in the nanoparticle core depending on the speed of cooling: (i) low; (ii) high.

We also found that there were nanoparticles composed of two nonparallel grains of eutectic crystals of Ag/Si (Fig. 2b). The electromagnetic field of these nanoparticles is formed of the vector sum of their components.

As distinguished from the formation mechanism of $TaSi_2$/Si nanoparticle [6,17], where the phase compounds are totally divided into two parts, the core of the Ag/Si nanoparticle undergoes mostly platelet

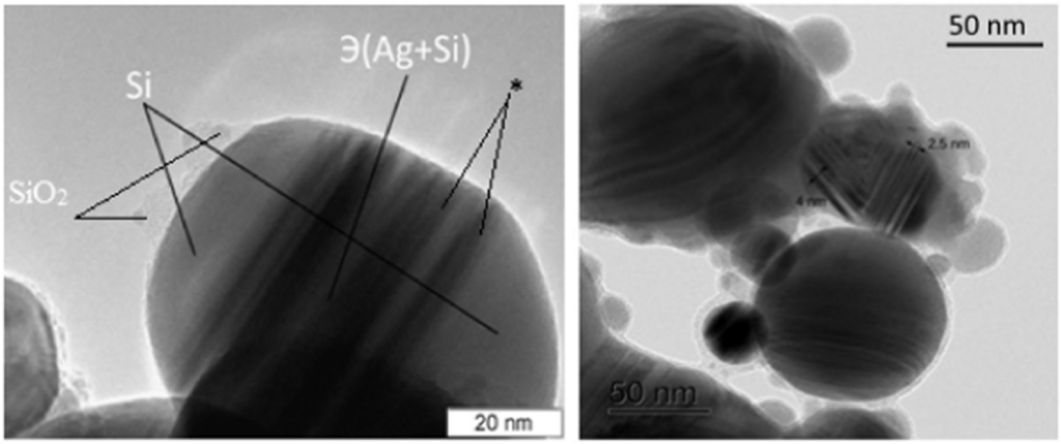

Fig. 2. (a) TEM image of the hypoeutectic nanoparticle Si + E(Si + Ag) * - showing the diffuse interface of the eutectic phases; (b) the different thicknesses of the diffraction fringes in the core.

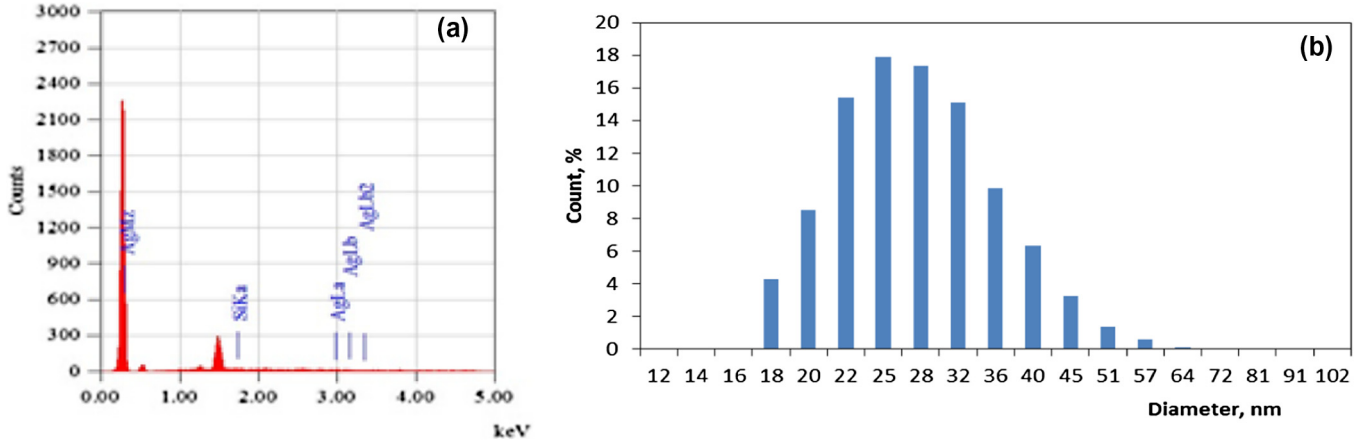

Fig. 4. Ag/Si particles after laser ablation: (a) quantitative EDS X-ray microanalysis showing the particles after laser ablation, consisting of Si (76.52 at.%), Ag (23.48 at.%); (b) the size distribution of the particles.

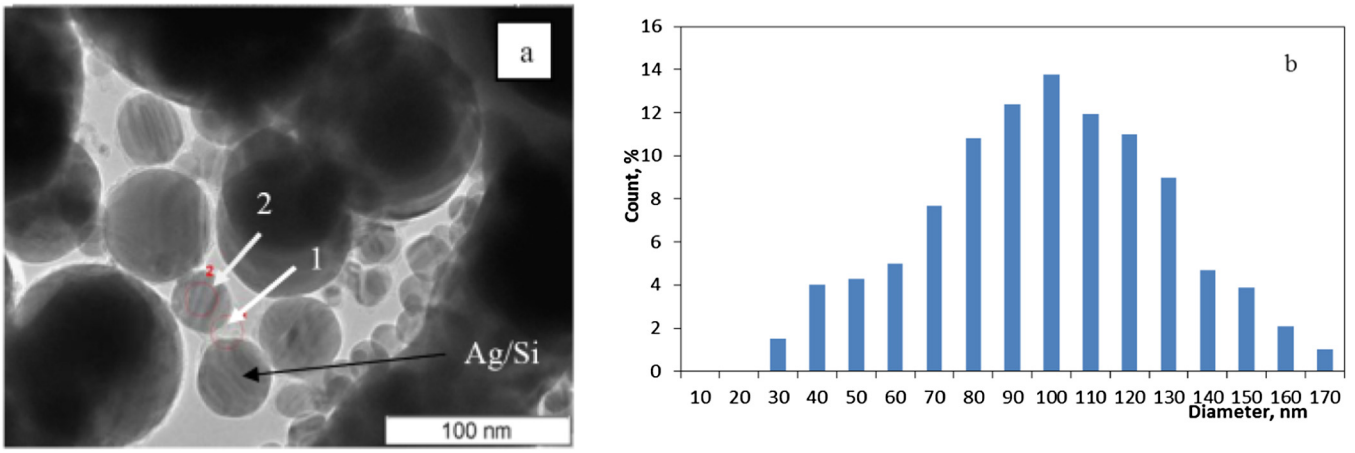

Fig. 5. Ag/Si particles after electron beam evaporation: (a) TEM. Arrows marked 1 and 2 show selected areas for SAED; Si (81.44 at.%) Ag (18.56 at.%) (b) The size distribution of the particles.

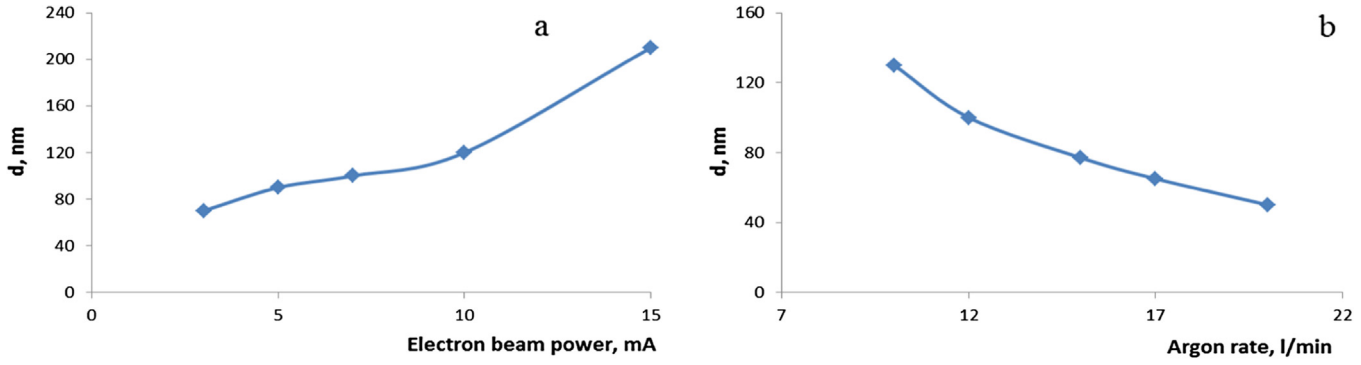

Fig. 6. Dependence of the average particle diameter on (a) the beam current; and (b) the flow rate of the inert gas.

decomposition. This is connected with the fact that platelet decomposition has counter moving of atoms for the formation of the equilibrium structure of the eutectic. The diffusion of phase boundaries in the core of the Ag/Si nanoparticle can be explained by the relatively high cooling rate (Fig. 2a, marked as *) when the silicon and silver do are not completely separated from each other in their pure form, meaning that a certain amount of the component that is “late” is fixed at the interface layer of the phase compounds. It is possible that in this case, the probability of charges arising at the phase boundary of the nanoparticle is lower or zero, unlike in nanoparticles with phase compounds Ag and Si that are fully divided and diffraction fringes with clearer outlines (for example, Fig. 7a).

Depending on the size and content of a stoichiometric droplet containing Ag, Si and O in different proportions and also on their cooling rates, the nanopowder consists of shell nanoparticles of Ag/Si@SiO_2 after crystallisation. We believe that this shell consists only of amorphous silica, which is formed in the process of desoxydation of silicon dioxide. All of the oxygen that is contained in the stoichiometric nanodroplets will be connected with silicon, which has a higher sensitivity to oxygen than the silver [16]. While cooling, silica will segregate at the surface due to the lower surface tension of silicon dioxide compared with silver or silicon [18,19]. After the formation of the silica

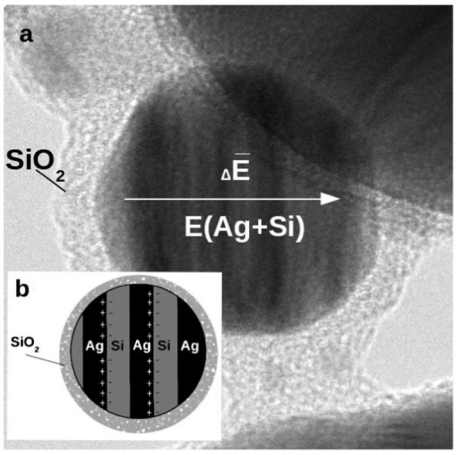

Fig. 7. Schematic image of a nanoparticle with eutectic core with a dipole moment: (a) the resulting electric field intensity of the nanoparticle $\Delta\bar{E}$ (TEMx150000); (b) a possible scheme for the charge separation between the conductor (Ag) and semiconductor (Si).

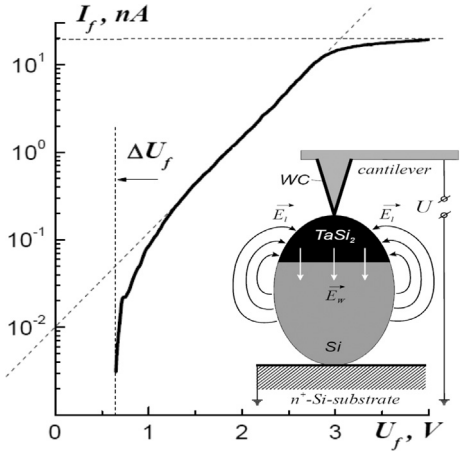

Fig. 8. I-V curve of the $TaSi_2$/Si nanoparticle and the electrical field scheme. The figure was constructed on the basis of data from [20,21].

shell, the oxygen will not take part in further structural formation of the nanoparticle core in the Ag-Si system [16]. Excess silicon or silver contained in the core of the nanoparticle will evolve in the form of primary crystals, and any that is left will evolve in the form of eutectic E (Si + Ag) (Fig. 3).

The structure of the core of the Ag/Si nanoparticle consists of alternating parallel platelets of silver and silicon. The possibility of charge polarization in these layers leads to the assumption that a material with high electric potential is formed. The strong polarisation properties of such nanoparticles are related to the charge separation in eutectics and the possible formation of the Shottky barrier at nanometre scale. Moreover, the field created by the space charge region may be larger than the size of the nanoparticle itself and have a complex shape, as shown above.

A similar situation for the formation of the Shottky barrier was obtained for Janus-like $TaSi_2$/Si nanoparticles [20,21]. A study of their conductivity using AFM (IPR method) showed the presence of nonlinear current-voltage characteristics (CVC) (Fig. 8). The linear section of the direct branch of the I–V characteristic recorded on a semi-log scale confirmed the presence of a potential Schottky barrier in the interface region, and its height was estimated as $\varphi_b \approx 0.4$ eV for a particle with diameter D = 100 nm [20]. Abnormally large values of the ideality index n were observed, caused by the nanometre contact diameter and the strong influence of the periphery E_l embedded in the contact field. The presence of the extended dead region $\varphi_b < \Delta U \approx 0.65$ V in the initial part of the I–V characteristic supported this conclusion. In [21], it was reported that the built-in electric field of the periphery contributed to a significant (several orders of magnitude) increase in the current (β_I) and volt (β_U) photosensitivity of metal-semiconductor contacts with a Schottky barrier.

The presence of these electrostatic fields in Janus-like nanoparticles may mean that their use in high-performance photoelectric converters and other practical applications is promising.

4. Conclusion

1. The formation mechanism of the diffraction fringes in the cores of nanoparticles of the system Ag-Si arises from eutectic decomposition into layers of silver and silicon.
2. The possibility of managing the size of the eutectic plates with the help of the cooling rate is demonstrated, which leads to a decrease or increase in their number and is of high practical value in altering the total potential of the nanoparticle. The cooling rate also determines the formation of layered or globular eutectic compounds.
3. The presence of a eutectic in the core of Ag-Si nanoparticle leads to the formation of electrical potential at the border between the metal and semiconductor layers.

Conflict of interest

The authors declare that there are no conflicts of interest.

Acknowledgments

This work was supported by the Russian Scientific Foundation [project number 18-79-10143].

References

[1] G.A. Sotiriou, A.M. Hir, P.-Y. Lozach, A. Teleki, F. Krumeich, S.E. Pratsinis, Chem. Mater. 23 (7) (2011) 1985–1992.
[2] X. Fu, J. Liu, H. Yang, J. Sun, X. Li, X. Zhang, Y. Jia, Mater. Chem. Phys. 130 (1–2) (2011) 334–339.
[3] N.M. Ravindra, L. Jin, D. Ivanov, V.R. Menta, L.M. Dieng, G. Popov, O.H. Gokce, J. Grow, A.T. Fiory, J. Electron. Mater. 31 (10) (2002) 1074–1079.
[4] G. Krishnan, M.A. Verheijen, G.H. ten Brink, G. Palasantzas, B.J. Kooi, Tuning structural motifs and alloying of bulk immiscible Mo–Cu bimetallic nanoparticles by gas-phase synthesis, Nanoscale 5 (2013) 5375–5383.
[5] A.V. Nomoev, S.P. Bardakhanov, Tech. Phys. Lett. 38 (4) (2012) 375–378.
[6] A.V. Nomoev, et al., Synthesis, characterization, and mechanism of formation of Janus-like nanoparticles of tantalum silicide-silicon ($TaSi_2$/Si), Nanomaterials 5 (1) (2014) 26–35.
[7] C. Langlois, Z.L. Li, J. Yuan, D. Alloyeau, J. Nelayah, D. Bochicchio, R. Ferrando, C. Ricolleau, Nanoscale 4 (2012) 3381–3388.
[8] Z. Swiatkowska-Warkocka, et al., Synthesis of new metastable nanoalloys of immiscible metals with a pulse laser technique, Sci. Rep. 5 (2015) 9849, , https://doi.org/10.1038/srep09849.
[9] Z. Swiatkowska-Warkocka, et al., Langmuir 28 (2012) 4903–4907.
[10] P. Grammatikopoulos, S. Steinhauer, J. Vernieres, V. Singh, M. Sowwan, Nanoparticle design by gas-phase synthesis, Adv. Phys.: X 1 (1) (2016) 81–100, https://doi.org/10.1080/23746149.2016.1142829.
[11] M. Lerner, A. Pervikov, E. Glazkova, N. Svarovskaya, A. Lozhkomoev, S. Psakhie, Powder Technol. 288 (2016) 371–378.
[12] J.-P. Palomares-Baez, E.E. Panizon, R. Ferrando, Nanoscale effects on phase separation, Nano Lett. 17 (9) (2017) 5394–5401, https://doi.org/10.1021/acs.nanolett.7b01994.
[13] B. Predel, H. Bankstahl, Thermodynamic properties of liquid Ag-Ge, Ag-Si, Au-Ge and Au-Si Alloys, J. Less-Common Met. 43 (1975) 191–203.
[14] A.P. Gulyaev, Metallurgy, Metallurgy, Moscow, 1977.
[15] A.P. Zavjalov, K.V. Zobov, V.V. Syzrantsev, S.P. Bardakhanov, I.K. Chakin, Synthesis of copper nanopowders using electron-beam evaporation at atmospheric pressure of inert gas, Nanotechnol. Russia 9 (11–12) (2014) 660–666.
[16] A.R. Radnaev, S.V. Kalashnikov, A.V. Nomoev, Nature of diffraction fringes originating in the core of core–shell nanoparticle Cu/SiO_2 and formation mechanism of the structures, Chem. Phys. Lett. 651 (2016) 274–277.
[17] A.V. Nomoev, et al., Thermodynamic considerations in the formation of Janus-like TaSi 2/Si nanoparticles by electron-beam evaporation, Chem. Phys. Lett. 637 (2015) 94–96.
[18] A. Nomoev, S. Bardakhanov, M. Schreiber, D. Bazarova, N. Romanov, B. Baldanov,

B. Radnaev, V. Syzrantsev, Structure and mechanism of formation of core-shell nanoparticles obtained by an evaporation-condensation method, Beilstein J. Nanotechnol. 6 (2015) 874–880.
[19] J. Temuujin, et al., Preparation of copper and silicon/copper powders by a gas evaporation-condensation method, Bull. Mater. Sci. 32 (5) (2009) 543–547.
[20] N.A. Torkhov, Nature of forward and reverse saturation currents in metal-semiconductor contacts with the Schottky barrier, Semiconductors 44 (6) (2010) 737–744.
[21] N.A. Torkhov, The influence of periphery electrostatic field upon the photovoltaic effect in metal−semiconductor contacts with Schottky barrier, Semiconductors 52 (10) (2018) 1269–1292.